

Non-convergence versus non-conservation in effective heat capacity methods for phase change problems

Zhen-Xiang Gong and Arun S. Mujumdar
Department of Chemical Engineering, McGill University,
Montreal, Quebec, Canada

Nomenclature

c	= specific heat	T_{mp}	= upper limit of melting temperature ($T_m+0.5\Delta T$)
c_{eff}	= effective specific heat ($\lambda/\Delta T$)	t	= time
$[C]$	= heat capacity matrix	x, y, z	= space co-ordinates
$[C_{ij}]$	= elements of heat capacity matrix	<i>Greek symbols</i>	
$\{F\}$	= heat load vector	Δt	= time step
F_j	= elements of heat load vector	ΔT	= phase change temperature interval
h	= convection heat transfer coefficient	Γ	= boundary
H	= enthalpy	λ	= latent heat
k	= thermal conductivity	ρ	= density
$[K]$	= conductance matrix	Ω	= solution domain
K_{ij}	= elements of conductance matrix	<i>Superscripts</i>	
n	= outward normal of boundary	e	= element
N_i, N_j	= shape function	i	= i th iteration
q	= heat flux due to conduction	n	= n th time step
Q	= rate of internal heat generation	<i>Subscripts</i>	
T	= temperature	l, j	= node number of an element
T_f	= ambient temperature	l	= liquid phase
T_i	= initial temperature	s	= solid phase
T_m	= melting temperature	t	= time t
T_{mn}	= lower limit of melting temperature ($T_m-0.5\Delta T$)	$t + \Delta t$	= time $t + \Delta t$

Note: The symbols defined above are subject to alteration on occasion

Introduction

To handle moving interfaces numerically in solving melting and solidification problems, two types of solution techniques have been developed. One is the time dependent grid method and the other is the fixed grid method. Because of their conceptual simplicity and ease of implementation, fixed grid approaches have found wide application. The essential feature of fixed grid approaches is that

Z.-X. Gong gratefully acknowledges the financial support of the Canadian International Development Agency (CIDA) and McGill University in the form of a McGill/CIDA Fellowship. Research support of the Natural Science and Engineering Council of Canada as well as the Exergex Corporation is also acknowledged.

the latent heat evolution is accounted for in the governing equation by defining either an enthalpy, or an effective specific heat, or a heat source. Consequently, the numerical solution can be carried out on a space grid that remains fixed throughout the calculation process.

In the original effective heat capacity method the latent heat effect is approximated by a large effective heat capacity over a small temperature range[1]. This approach is simple in concept and easy to implement. Unfortunately, however, it is so sensitive to the choice of the phase change temperature interval and time integration scheme that in some cases the correct solution or even a solution cannot be obtained owing to non-convergence caused by the abrupt change of specific heat at the interface. Many improved versions of this approach have been reported over the last two decades (e.g. Comini *et al.*[2], Morgan *et al.*[3], Guidice *et al.*[4], Lemmon[5], Pham[6] and Comini *et al.*[7]). These improved versions have been well established and are effective in solving a wide range of conduction phase change problems. However, in the authors' experience, non-convergence sometimes occurs when these approaches are implemented with implicit iterative time integration schemes and a large time step is used, e.g. the Lemmon scheme[5]. Swaminathan and Voller[8] reported a source based method to deal with phase change problems. Their scheme is strictly conservative and computationally efficient.

In this paper, the cause and cure of non-convergence in effective heat capacity methods are presented. Based on the energy conservation law, the transient semi-discretized governing equation based on the original effective heat capacity method is reformulated.

Mathematical formulation

Let us take the original effective heat capacity method[1] for illustration. The governing equation for phase change heat conduction based on this method can be described by:

$$\frac{\partial(\rho c T)}{\partial t} = \frac{\partial}{\partial x} \left(k \frac{\partial T}{\partial x} \right) + \frac{\partial}{\partial y} \left(k \frac{\partial T}{\partial y} \right) + \frac{\partial}{\partial z} \left(k \frac{\partial T}{\partial z} \right) + Q \quad (1)$$

in which

$$\rho, c, k = \begin{cases} \rho, & c_s, & k_s, & T \leq T_m - 0.5\Delta T \\ \rho, & \frac{\lambda}{\Delta T}, & (1-f)k_s + fk_l, & T_m - 0.5\Delta T < T < T_m + 0.5\Delta T \\ \rho, & c_l, & k_l, & T \geq T_m + 0.5\Delta T \end{cases} \quad (2)$$

Finite element formulation

After spacewise discretization of equation (1), subject to the boundary condition of the third kind (convection boundary condition), viz.

$$-k \frac{\partial T}{\partial n} = h(T - T_f), \quad (3) \quad \text{Heat capacity methods}$$

being accomplished using the standard Galerkin method[9], we obtain the following semi-discrete matrix system:

$$[C]\{\dot{T}\} + [K]\{T\} = \{F\} \quad (4) \quad \underline{\underline{567}}$$

in which the superposed dot denotes differentiation with respect to time. Typical elements of the matrices in equation (4) are

$$C_{IJ} = \sum_{\Omega} \rho c N_I N_J d\Omega, \quad (5)$$

$$K_{IJ} = \sum_{\Omega} k \left(\frac{\partial N_I}{\partial x} \frac{\partial N_J}{\partial x} + \frac{\partial N_I}{\partial y} \frac{\partial N_J}{\partial y} + \frac{\partial N_I}{\partial z} \frac{\partial N_J}{\partial z} \right) d\Omega + \sum_{\Gamma} h N_I N_J d\Gamma, \quad (6)$$

$$F_I = \sum_{\Omega} Q N_I d\Omega + \sum_{\Gamma} h T_f N_I d\Gamma. \quad (7)$$

It is reiterated that the set of equations (4) is highly non-linear owing to the abrupt change of specific heat and the thermal conductivity when phase change takes place.

A lumped mass model[6,9] is used to calculate the heat capacity matrix [C]. The stabilized one-point quadrature algorithm[10,11] is employed to compute the conductance matrix [K] and the heat load vector {F}.

The discretization of the time derivative in equation (4) is most often achieved with a finite difference technique. Although many time-stepping schemes are available, the most popular ones are two-time-level methods in which iterations are required within each time step. Here we use backward Euler procedure, viz.

$$\{\dot{T}\} = \left\{ \frac{T_{t+\Delta t} - T_t}{\Delta t} \right\}. \quad (8)$$

According to this scheme, equation (4) can be approximated as:

$$[C + \Delta t K]\{T_{t+\Delta t}\} = [C]\{T_t\} + \{F\} \quad (9)$$

Problem and cause analysis

A converged solution cannot be obtained with equation (9) even if a very large value for the phase change temperature interval is assumed. Why does equation (9) not converge? In the following we will analyse the cause.

Let us take a melting process for example. In order to clarify the explanation, equation (9) is rewritten in a point form. For point *l*,

$$(C_l + K_H)T_{t+\Delta t} = \sum_{j \neq l} K_{lj}(T_j)_{t+\Delta t} + C_l T_t + F_l \quad (10)$$

According to the implicit scheme rules, the values of C_l , K_{lj} , and F_l should be updated with the latest temperature $T_{t+\Delta t}^{i-1}$. Assume point l enters phase change from solid state during the time interval, t to $t + \Delta t$, and $T_{t+\Delta t}^{i-1} < T_{mn}$ ($T_m - 0.5\Delta T$) and $T_{t+\Delta t}^i > T_{mn}$. At iteration i , c_l takes on the value of c_s and there is $T_{t+\Delta t}^i > T_{mn}$. $T_{t+\Delta t}^i$ has two possible situations. One is $T_{mn} < T_{t+\Delta t}^i < T_{mp}$ ($T_m + 0.5\Delta T$) and the other is $T_{t+\Delta t}^i > T_{mp}$. The latter case occurs when the phase change temperature interval is very small or the time step is very large or both. For the latter case phase change is stepped over in an iteration and latent heat effect is not taken into account. A false solution is therefore reached.

For the former case the following will happen. At iteration $i + 1$, c_l takes on the value of c_{eff} ($\lambda/\Delta T$) and C_l becomes a very large number correspondingly since c_{eff} is in general a very large value. Compared with this large value of C_l , relative contributions of the other terms to equation (10) can be neglected. Therefore, equation (10) becomes:

$$C_l T_{t+\Delta t}^{i+1} \approx C_l T_t \quad (11)$$

and therefore, $T_{t+\Delta t}^{i+1} \approx T_t < T_{mn}$. In this case $T_{t+\Delta t}^{i+1}$ is dragged back to a temperature in solid state, and then an iteration $i+2$, c_l takes on the value of c_s again. This results in $T_{mn} < T_{t+\Delta t}^{i+2} < T_{mp}$. At iteration $i+3$, the same situation as iteration $i+1$ occurs. This explains why a converged solution can never be obtained.

Even if the phase change temperature interval is assumed to be a very large value, c_{eff} is still in general tens, or even hundreds, of times larger than c_s or c_l . Therefore, such temperature oscillations as described above cannot be avoided.

What is the true value of temperature $T_{t+\Delta t}^{i+1}$? Since the real process is that at iteration i the control volume has already entered the melting state, $T_{t+\Delta t}^{i+1}$ should be in the the range of the melting temperature interval, i.e. $T_{mn} < T_{t+\Delta t}^{i+1} < T_{mp}$.

Why do the above mentioned temperature oscillations occur? This is owing to the non-conservative behaviour caused by the abrupt change of specific heat in the time interval of t to $t + \Delta t$. In the following, we will reformulate the heat transfer process based on the basic energy conservation law. After the correct formulations are obtained, the non-conservation behaviour will be seen clearly.

In the Lemmon scheme[5], the effective specific heat is calculated as follows:

$$c_{eff} = \left(\frac{\nabla H \cdot \nabla H}{\nabla T \cdot \nabla T} \right)^{1/2} \quad (12)$$

Similar temperature oscillation in the Lemmon scheme to that described above occasionally occurs as it is implemented with an implicit iteration time integration scheme and the time step exceeds a certain limit. This will be shown in the illustrative examples.

A conservative scheme

Here let us model a one-dimensional melting process for illustration. Assume a control volume dx (see Figure 1) is in solid state at time t , and at time $t+\Delta t$ it has entered molten state. During the time interval Δt the net thermal energy flowing into the control volume by conduction is:

$$\int_t^{t+\Delta t} [q - (q + \frac{\partial q}{\partial x} dx)] dt = - \int_t^{t+\Delta t} \frac{\partial q}{\partial x} dx dt \tag{13}$$

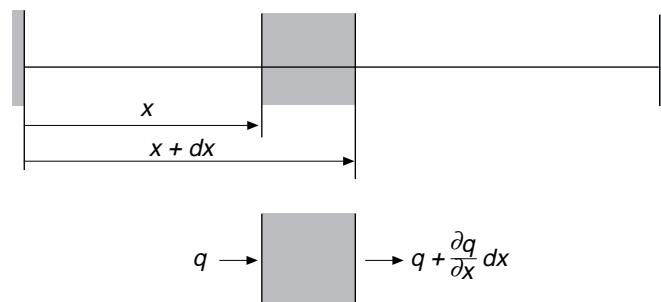


Figure 1.
Physical model

The thermal energy is absorbed by the material heat capacity and there is, therefore, a temperature rise in the control volume. Thermal energy absorbed by the control volume (see Figure 2) is:

$$[\rho c_s (T_{mn} - T_t) + \rho c_{eff} (T_{t+\Delta t} - T_{mn})] dx \tag{14}$$

According to the energy conservation law we obtain:

$$[\rho c_s (T_{mn} - T_t) + \rho c_{eff} (T_{t+\Delta t} - T_{mn})] dx = - \int_t^{t+\Delta t} \frac{\partial q}{\partial x} dt dx \tag{15}$$

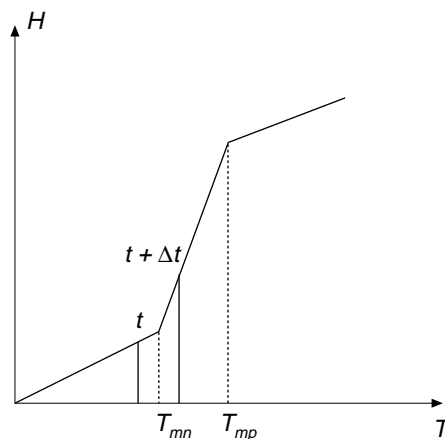


Figure 2.
Illustration of the heat transfer process in the $H-T$ curve

Since

$$\frac{\partial q}{\partial x} = -k \frac{\partial T}{\partial x} \quad (16)$$

equation (14) becomes

$$\rho c_s (T_{mn} - T_i) + \rho c_{eff} (T_{t+\Delta t} - T_{mn}) = \int_t^{t+\Delta t} \frac{\partial}{\partial x} \left(k \frac{\partial T}{\partial x} \right) dt \quad (17)$$

From equation (16) it can be seen clearly that it is not conservative for the specific heat of the control volume to take the value of either c_s or c_{eff} during the time interval in which phase change takes place.

The above mentioned non-conservation behaviour occurs in the time interval not only when the control volume starts to enter melting, but also when the control volume gets out of the phase change. When a control volume gets out of phase change during the time interval, t to $t + \Delta t$, the correct governing equation is:

$$\rho c_{eff} (T_{mp} - T_i) + \rho c_l (T_{t+\Delta t} - T_{mp}) = \int_t^{t+\Delta t} \frac{\partial}{\partial x} \left(k \frac{\partial T}{\partial x} \right) dt \quad (18)$$

For the case where the temperature of the control volume steps over the phase change interval during the time interval, t to $t + \Delta t$ the correct governing equation is:

$$\rho c_s (T_{mn} - T_i) + \rho c_{eff} (T_{mp} - T_{mn}) + \rho c_l (T_{t+\Delta t} - T_{mp}) = \int_t^{t+\Delta t} \frac{\partial}{\partial x} \left(k \frac{\partial T}{\partial x} \right) dt \quad (19)$$

For the case of freezing, similar formulations can be obtained. They are:

$$\rho c_l (T_{mp} - T_i) + \rho c_{eff} (T_{t+\Delta t} - T_{mp}) = \int_t^{t+\Delta t} \frac{\partial}{\partial x} \left(k \frac{\partial T}{\partial x} \right) dt \quad (20)$$

for entering phase change;

$$\rho c_{eff} (T_{mn} - T_i) + \rho c_s (T_{t+\Delta t} - T_{mn}) = \int_t^{t+\Delta t} \frac{\partial}{\partial x} \left(k \frac{\partial T}{\partial x} \right) dt \quad (21)$$

for exiting phase change; and

$$\rho c_l (T_{mp} - T_i) + \rho c_{eff} (T_{mn} - T_{mp}) + \rho c_s (T_{t+\Delta t} - T_{mn}) = \int_t^{t+\Delta t} \frac{\partial}{\partial x} \left(k \frac{\partial T}{\partial x} \right) dt \quad (22)$$

for stepping over phase change in a time interval Δt .

For a time interval when there is no switch of states, the governing equation is

$$\rho c (T_{t+\Delta t} - T_i) = \int_t^{t+\Delta t} \frac{\partial}{\partial x} \left(k \frac{\partial T}{\partial x} \right) dt \quad (23)$$

in which c is updated with equation (2).

The reformulated governing equations are exactly conservative. As will be seen in the test examples, temperature oscillation which results in non-convergence is completely eliminated and the new scheme has no limitation on selection of the phase change temperature interval.

The Newton-Raphson method is used to solve the resulting algebraic equation system. The convergence criteria selected are that the Cartesian norms of both the increment of temperature rate and the residual of the algebraic equation system are each less than a small constant, e.g. 1.0×10^{-6} .

Implementation

Taking the melting case for illustration, four cases are required to distinguish the implementation of the newly proposed scheme.

- (1) if $T_t < T_{mn}$ and $T_{t+\Delta t}^i < T_{mn}$ or $T_t > T_{mp}$ and $T_{t+\Delta t}^i > T_{mp}$, equation (23) is used;
- (2) if $T_t < T_{mn}$ and $T_{mn} < T_{t+\Delta t}^i < T_{mp}$, equation (17) is used;
- (3) If $T_{mn} < T_t < T_{mp}$ and $T_{t+\Delta t}^i > T_{mp}$, equation (18) is used;
- (4) if $T_t < T_{mn}$ and $T_{t+\Delta t}^i < T_{mp}$ equation (19) is used.

No special treatment is required in the solution iteration process except for checking the temperature of the element nodes at each iteration and adopting the corresponding equation according to the temperature of the element node.

Illustrative examples

To demonstrate the accuracy and efficiency of the new conservative scheme, solutions of four illustrative problems are presented. All the computations were carried out by a Pentium 100 MHz.

Problem 1: Solidification of a semi-infinite slab of a liquid – constant thermal properties

A liquid initially at a uniform temperature, 10°C , which is above its freezing point (0°C) is confined to a half-space $x > 0$. At time $t = 0$, the boundary surface at $x = 0$ is lowered to a temperature, -20°C and maintained at this temperature for $t > 0$. The thermophysical properties are as follows:

$$k_s = k_l = 2.22 \text{ W/m.K}, c_s = c_l = 1,762 \text{ J/kg.K}, \rho = 1,000 \text{ kg/m}^3, \lambda = 338,000 \text{ J/kg}, T_m = 0^\circ\text{C}.$$

Two-dimensional elements are utilized to solve this problem although it is physically one-dimensional. The finite element mesh is displayed in Figure 3 in which $BC = 1.0\text{m}$. A phase change temperature interval of 1.0×10^{-10} is used for the computations in this test problem.

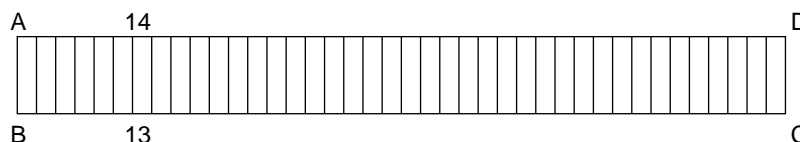


Figure 3.
Finite element mesh

HFF
7,6

572

The Stefan number of this test problem is 0.104. Computations were carried out using the optimal source based scheme of Swaminathan and Voller[8] (SV scheme) as well as the scheme described above (GM scheme) with 40 elements and a time step of 1,000 seconds. A total of 300 time steps is required to complete each run for this problem. The convergence criteria are specified to be 1.0×10^{-6} . As the computed slab domain is finite, comparison with the theoretical infinite slab solution must be terminated when the temperature begins to change appreciably at boundary DC. Table I shows a comparison of the performance of the two schemes.

Table I.
Performance of methods for one-dimensional test problem (small Stefan number)

	Freezing front at $t = 3.0 \times 10^5$ seconds (m)	Total number of iterations	CPU time (seconds)
Exact solution	0.2551		
GM scheme	0.2533	619	16.4
SV scheme	0.2527	610	16.2

The same solidification problem is also computed with a large Stefan number of 1.04. In this problem all parameters are the same as those in the last problem except for $\lambda = 33,800$ J/kg which is only one-tenth of that in the last problem. The time step used in this computation is 150 seconds. Table II shows a comparison of the performance of the GM and SV schemes.

Table II.
Performance measures for one-dimensional test problem (large Stefan number)

	Freezing front at $t = 4.5 \times 10^4$ seconds (m)	Total number of iterations	CPU time (seconds)
Exact solution	0.2261		
GM scheme	0.2245	617	16.5
SV scheme	0.2239	609	16.4

From Tables I and II it can be seen that the accuracy and the computational efficiency of the GM scheme and the SV scheme are almost the same.

Problem 2: Solidification of a semi-infinite slab of a liquid – discontinuous thermal properties

As in Problem 1 we used a Stefan number of 0.104. All other parameters are the same as those in Problem 1 except for the thermal conductivities and the specific heats of the phase change material. These thermophysical properties are as follows:

$$k_s = 2.22 \text{ W/m.K}, k_l = 0.556 \text{ W/m.K}, c_s = 1,762 \text{ J/kg.K}, c_l = 4,226 \text{ J/kg.K},$$

Computations were carried out using the Lemmon scheme (equation (12)), the optimal source based scheme of Swaminathan and Voller[8] (SV scheme) as well as the scheme described here (GM scheme) with 40 elements and a time step of 1,000 seconds. A total of 300 time steps is required for each run of this problem. A phase change temperature interval of 1.0×10^{-10} is used for the computations in this test problem.

The implicit rule is used to update the thermophysical properties in the solution iteration process. When phase change is taking place in one or more nodes in an element the thermal conductivity of the element is calculated as follows:

$$k_e = \frac{1}{nen} \sum_{i=1}^{nen} k_i; \quad (24)$$

in which nen is the total node number of an element. The thermal conductivity of an element node is updated directly according to the node temperature using linear interpolation.

Table III shows a comparison of the computational efficiency with these three schemes. From this table it can be seen that the computational efficiencies of the GM and the SV schemes are at the same level for this test problem.

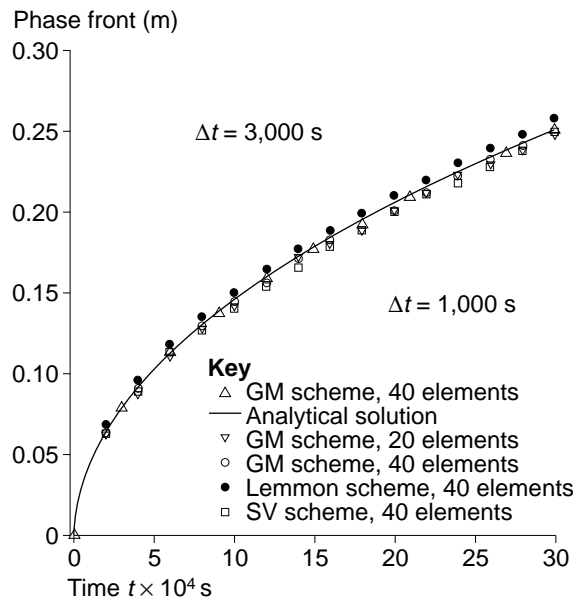
	Total number of iterations	CPU time (seconds)	Total number of iterations	CPU time (seconds)
Convergence criteria	1.0×10^{-6}		1.0×10^{-8}	
GM scheme	619	16.7	619	16.9
Lemmon scheme	679	18.5	977	27.5
SV scheme	610	18.2	610	18.1

Table III.
Comparison of computational efficiency

Figure 4 displays the computed freezing front progress using these three schemes and compares the results with the analytical solution[12]. It can be seen from this figure that the GM scheme has better agreement with the analytical solution than do the Lemmon and SV schemes. Also shown in this figure is the result using 20 elements and a time step of 1,000 seconds. It can be seen that the result is more accurate using the GM scheme even with half the number of the meshes used with the Lemmon and SV schemes. It should be noted that if a more complicated approach (Kirchoff approximation)[13] is used to treat the discontinuous thermal conductivity the accuracy of the prediction by the SV model is the same level as that by the GM model.

Numerical experiments showed that non-convergence occurs at time step 91 using the Lemmon scheme when the time step is increased to 1,100 seconds. This is caused by the temperature oscillation at nodes 13 and 14 which are the

Figure 4.
Comparison of the
computed interface
position with the
analytical solution



junctions of elements 6 and 7. The temperatures at nodes 13 and 14 oscillate from 0.5007 to -0.6626 iteration by iteration and convergence cannot be reached. An insight into the computation process determined that when the temperatures oscillate from 0.5007 to -0.6626 the effective specific heat of element 6 oscillates from 106,562.6 J/kg.K to 4,226 J/kg.K (specific heat of the liquid phase) and that of element 7 from 1,762 J/kg.K (specific heat of the solid phase) to 159,043.6 J/kg.K. The oscillation of the element specific heat results in a jump in the value of the effective specific heat of nodes 13 and 14 (from 54,162.3 J/kg.K to 81,634.8 J/kg.K). This jump leads to non-conservation of the final algebraic equations for points 13 and 14. A similar explanation can be given for such observations made on the original effective heat capacity method described previously.

Numerical experiments also showed that convergence can be reached even with a very large time step, e.g. 3,000 seconds, and that the accuracy does not degrade with the new conservative scheme. From Figure 4 it can be seen that the results using a time step of 3,000 seconds are in very good agreement with the analytical solution.

Problem 3. Solidification of a corner region

The corner region of a liquid body extending in the positive x and y -directions is frozen by bringing the surface temperature to -1.0°C at time $t = 0$. The thermophysical properties are $k_s = k_l = 1.0$ W/m.K, $c_s = c_l = 1.0$ J/kg.K, $\rho = 1.0$ kg/m³, $T_m = 0^\circ\text{C}$, $\lambda = 0.25$ J/kg and the initial condition is $T_i = 0.3^\circ\text{C}$. The phase change temperature interval is specified to be 1.0×10^{-10} K. 20×20 elements with a time step of 0.001 second are employed. A total of 500 time steps is required to complete each run for this problem. The finite element mesh is shown in Figure 5.

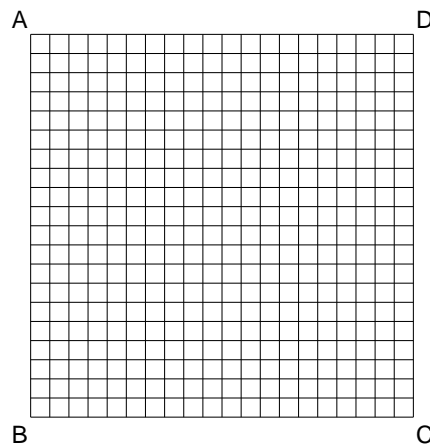


Figure 5.
Finite element mesh

Computations were also carried out using the Lemmon scheme, the optimal source based scheme of Swaminathan and Voller (SV scheme) as well as the scheme proposed in this study (GM scheme). With the time step of 0.001 seconds, the Lemmon scheme does not converge. A converged solution cannot be obtained until the time step size is decreased to 0.0002 seconds. Table IV shows a comparison of the average number of iterations required per time step between the SV scheme and the GM scheme. It is found that the computational efficiencies of the GM and the SV schemes are almost the same.

	Total number of iterations	CPU time (seconds)	Total number of iterations	CPU time (seconds)
Convergence criteria	1.0×10^{-6}		1.0×10^{-8}	
GM scheme	1,163	228.4	1,163	228.4
SV scheme	1,092	222.9	1,092	222.9

Table IV.
Comparison of computational efficiency

Figure 6 presents the results of the GM and SV schemes and compares them with the analytical solution[14] for the freezing front. It is found that the result of the GM scheme is in good agreement with the analytical solution and is identical to that of the SV scheme.

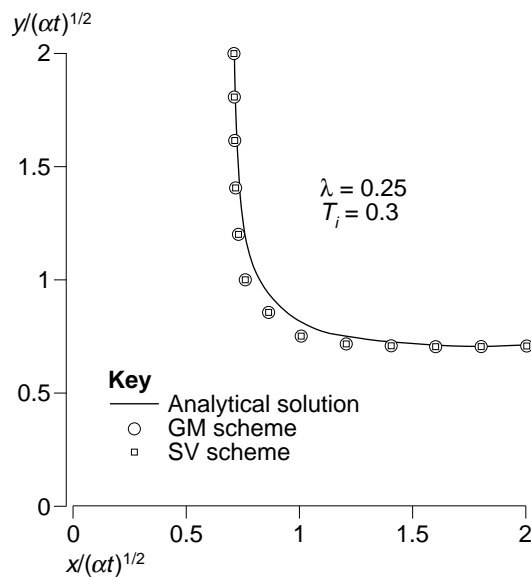
Problem 4

The geometry of the phase change material is a slice with a radius of 5cm as shown in Figure 6. The material is initially at a uniform temperature of 20°C with side AB and AC insulated. On the circumferential side, BC, there is heat convection with the heat transfer coefficient varying linearly, from 17.5 to 87.5

HFF
7,6

576

Figure 6.
Comparison of the
computed interface
position with the
analytical solution



W/m^2 , from point B to point C. The ambient temperature is $-23.6^\circ C$. The thermophysical parameters are as follows:

$$k_s = 1.55 \text{ W/m.K}, k_l = 0.5 \text{ W/m.K}, c_s = 1,240 \text{ J/kg.K}, c_l = 2,370 \text{ J/kg.K}, \rho = 960 \text{ kg/m}^3, \lambda = 167,400 \text{ J/kg}, T_m = -1.8^\circ C.$$

Computations were carried out using 300 elements and 331 nodes. A total of 2,000 time steps is required to complete each run for this problem. The finite element meshes are illustrated in Figure 7. The computed cases are listed in Table V and compared with the performance of the SV scheme.

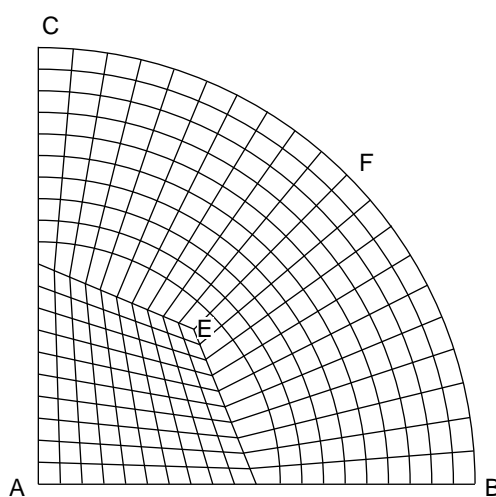


Figure 7.
Finite element mesh

From Table V it can be seen that for both large and very small phase change temperature intervals the iteration numbers and the computing time are almost the same between using the GM scheme and the SV scheme. This means that the computational efficiencies of the two schemes are on the same level. Numerical experiments also found that the Lemmon scheme does not converge until the time step is decreased to two seconds.

Convergence criteria Case	Δt (s)	1.0×10^{-6} ΔT (K)	GM scheme		SV scheme	
			Total number of iterations	CPU time (seconds)	Total number of iterations	CPU time (seconds)
1	5	1.0×10^{-10}	4,847	751.2	4,547	782.9
2	5	2.0	5,784	950.3	5,752	992.0

Table V.
Comparison of computational efficiency

Figures 8 and 9 display the temperature histories of points A, E and F for cases 1 and 2 respectively. The solid lines in the two figures are for the GM scheme and the dashed lines for the SV scheme. It can be seen that the predicted results are in very good agreement between the two schemes.

Also shown in Figures 8 and 9 are the results using the GM scheme with a time step of 100 seconds; these are represented by the dashed lines. It can be seen that the differences of the results between the time step sizes of 5 and 100 seconds are very small. Hence for the problems tested it appears that the new scheme is relatively insensitive to the choice of time step.

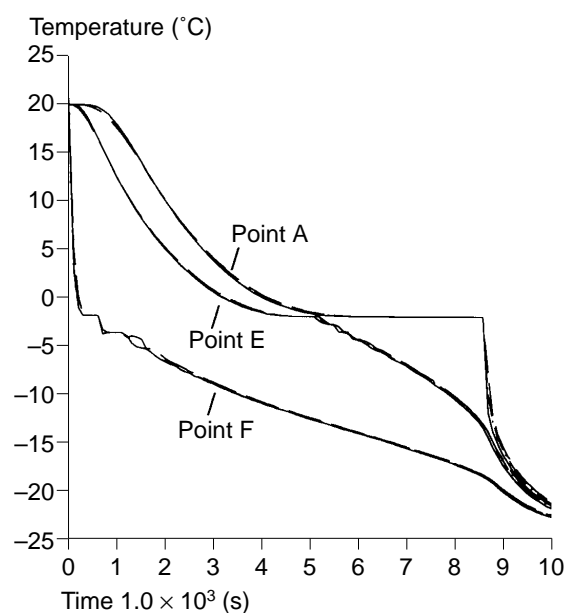
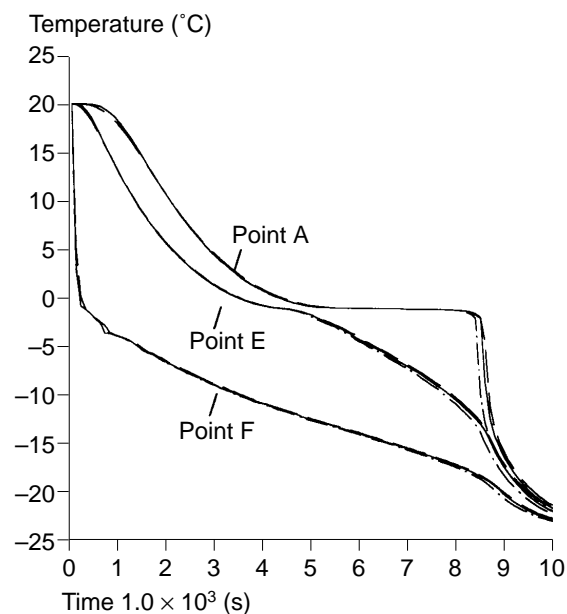


Figure 8.
Temperature histories
($\Delta T = 1.0 \times 10^{-10}$ K;
solid line for $\Delta t = 5$
seconds; dashed line for
 $\Delta t = 100$ seconds;
dash-and-dot line for
SV scheme)

Figure 9.
Temperature histories
($\Delta T = 2$ K; solid line for
 $\Delta t = 5$ seconds; dashed
line for $\Delta t = 100$
seconds; dash-and-dot
line for SV scheme



Concluding remarks

The cause of non-convergence resulting from temperature oscillation in effective heat capacity methods for phase change problems has been analysed. Based on the basic conservation law a new scheme was developed for the numerical solution of phase change problems. This scheme eliminates occurrence of non-convergence as well as false solutions. It is simple, easy to implement, and does not have limitations in the choice of the phase change temperature interval. Although it is implemented with the backward Euler time integration scheme, extension to other time schemes is direct. Numerical examples have demonstrated the effectiveness and the efficiency of the new scheme.

References

1. Bonacina, C., Comini, G., Fasano, A. and Primicero, M., "Numerical solution of phase-change problems", *Int. J. Heat Mass Transfer*, Vol. 16, 1973, pp. 1825-32.
2. Comini, G., Guidice, S.D., Lewis, R.W. and Zienkiewicz, O.C., "Finite element solution of non-linear heat conduction problems with reference to phase change", *Int. J. Numer. Meths. Engrg*, Vol. 8, 1974, pp. 613-24.
3. Morgan, K., Lewis, R.W. and Zienkiewicz, O.C., "An improved algorithm for heat conduction problems with phase change", *Int. Numer. Meths. Engrg*, Vol. 12, 1978, pp. 1191-5.
4. Guidice, S.D., Comini, G. and Lewis, R.W., "Finite element simulation of freezing processes in soil", *Int. J. Numer. Anal. Meths. Geomech*, Vol. 2, 1978, pp. 223-35.
5. Lemmon, E.C., "Multidimensional integral phase change approximations for finite element conduction codes", in Lewis, R.W., Morgan, K. and Zienkiewicz, O.C. (Eds), *Numerical Methods in Heat Transfer*, Wiley, Chichester, 1981, pp. 201-13.

-
6. Pham, Q.T., "The use of lumped capacitance in the finite-element solution of heat conduction problems with phase change", *Int. J. Heat Mass Transfer*, Vol. 29, 1986, pp. 285-91.
 7. Comini, G., Guidice, S.D. and Saro, O., "A conservative algorithm for multidimensional conduction phase change", *Int. Numer. Meths. Engrg*, Vol. 30, 1990, pp. 697-709.
 8. Swaminathan, C.R. and Voller, V.R., "On the enthalpy method", *Int. Num. Meth. Heat Fluid Flow*, Vol. 3, 1993, pp. 233-44.
 9. Zienkiewicz, O.C. and Taylor, R.L., *The Finite Element Method*, 4th ed., Vol. 1, McGraw-Hill, London, 1989.
 10. Liu, W.K. and Belytschko, T., "Efficient linear and non-linear heat conduction with a quadrilateral element", *Int. J. Numer. Meths. Engrg*, Vol. 20, 1984, pp. 931-48.
 11. Gong, Z.X. and Mujumdar, A.S., "A simultaneous iteration procedure for the finite element solution of the enthalpy model for phase change heat conduction problems", *Int. J. Num. Meth. Heat Fluid Flow*, Vol. 5, 1994, pp. 589-600.
 12. Luikov, A.V., *Analytical Heat Diffusion Theory*, Academic Press, New York, NY, 1968.
 13. Voller, V.R. and Swaminathan, C.R., "Treatment of discontinuous thermal conductivity in control-volume solutions of phase-change problems", *Numerical Heat Transfer, Part B*, Vol. 24, 1993, pp. 161-80.
 14. Budhia, H. and Kreith, F., "Heat transfer with melting or freezing in a wedge", *Int. J. Heat Mass Transfer*, Vol. 16, 1973, pp. 195-211.